20 contiguous voxels. Brain regions were estimated from Talairach and Tournoux[30], after adjustments for differences between MNI and Talairach coordinates. To evaluate the intersubjectconsistency of brain activations associated with normal and impaired reading in Chinese, we created penetrance maps by combining binary individual functional maps[31]. Penetrance maps were then overlaid on axial views of T_1-weighted images to demonstrate the voxels with significant activation in three or more subjects. The binary functional maps were determined using $P < 0.05$ corrected for each subject.

Received 5 April; accepted 13 July 2004; doi:10.1038/nature02865.

1. Eden, G. & Moats, L. The role of neuroscience in the remediation of students with dyslexia. *Nature Neurosci.* **5,** 1080–1084 (2002).
2. Horwitz, B., Rumsey, J. M. & Donohue, B. C. Functional connectivity of the angular gyrus in normal reading and dyslexia. *Proc. Natl Acad. Sci. USA* **95,** 8939–8944 (1998).
3. Temple, E. *et al.* Neural deficits in children with dyslexia ameliorated by behavioral remediation: Evidence from functional MRI. *Proc. Natl Acad. Sci. USA* **100,** 2860–2865 (2003).
4. Shaywitz, S. E. *et al.* Functional disruption in the organization of the brain for reading in dyslexia. *Proc. Natl Acad. Sci. USA* **95,** 2636–2641 (1998).
5. Aylward, E. H. *et al.* Instructional treatment associated with changes in brain activation in children with dyslexia. *Neurology* **61,** 212–219 (2003).
6. Turkeltaub, P. E., Gareau, L., Flowers, D. L., Zeffiro, T. & Eden, G. Development of neural mechanisms for reading. *Nature Neurosci.* **6,** 767–773 (2003).
7. Rayner, K., Foorman, B. R., Perfetti, C. A., Pesetsky, D. & Seidenberg, M. S. How psychological science informs the teaching of reading. *Psychol. Sci. Publ. Interest* **2,** 31–74 (2001).
8. Paulesu, E. *et al.* Dyslexia: cultural diversity and biological unity. *Science* **291,** 2165–2167 (2001).
9. Tan, L. H. *et al.* The neural system underlying Chinese logograph reading. *Neuroimage* **13,** 836–846 (2001).
10. Tan, L. H. *et al.* Neural systems of second language reading are shaped by native language. *Hum. Brain Mapp.* **18,** 158–166 (2003).
11. Siok, W. T., Jin, Z., Fletcher, P. & Tan, L. H. Distinct brain regions associated with syllable and phoneme. *Hum. Brain Mapp.* **18,** 201–207 (2003).
12. Mattingly, I. G. in *Language by Ear and by Eye: The Relationships Between Speech and Reading* (eds Kavanagh, J. F. & Mattingly, I. G.) 133–147 (MIT Press, Cambridge, Massachusetts, 1972).
13. Wang, W. S.-Y. The Chinese language. *Sci. Am.* **228,** 50–62 (1973).
14. Perfetti, C. A. & Tan, L. H. in *Reading Chinese Script: A Cognitive Analysis* (eds Wang, J., Inhoff, A. W. & Chen, I.) 115–134 (Lawrence Erlbaum Associates, Mahwah, New Jersey, 1999).
15. Perfetti, C. A., Liu, Y. & Tan, L. H. The lexical constituency model: Some implications of research on Chinese for general theories of reading. *Psychol. Rev.* (in the press).
16. Price, C. J., More, C. J., Humphreys, G. W. & Wise, R. S. J. Segregating semantic from phonological processes during reading. *J. Cogn. Neurosci.* **9,** 727–733 (1997).
17. Gabrieli, J. D., Poldrack, R. A. & Desmond, J. E. The role of left prefrontal cortex in language and memory. *Proc. Natl Acad. Sci. USA* **95,** 906–913 (1998).
18. Courtney, S. M., Petit, L., Maisog, J. M., Ungerleider, L. G. & Haxby, J. V. An area specialized for spatial working memory in human frontal cortex. *Science* **279,** 1347–1351 (1998).
19. D'Esposito, M. *et al.* The neural basis of the central executive system of working memory. *Nature* **378,** 279–281 (1995).
20. Petrides, M., Alivisatos, B., Meyer, E. & Evans, A. C. Functional activation of the human frontal cortex during the performance of verbal working memory tasks. *Proc. Natl Acad. Sci. USA* **90,** 878–882 (1993).
21. Cohen, L. *et al.* The visual word form area: spatial and temporal characterization of an initial stage of reading in normal subjects and posterior split-brain patients. *Brain* **123,** 291–307 (2000).
22. Tan, L. H. *et al.* Brain activation in the processing of Chinese characters and words: A functional MRI study. *Hum. Brain Mapp.* **10,** 16–27 (2000).
23. Gold, B. T. & Buckner, R. L. Common prefrontal regions coactivate with dissociable posterior regions during controlled semantic and phonological tasks. *Neuron* **35,** 803–812 (2002).
24. Wagner, A. D., Pare-Blagoev, J. E., Clark, J. & Poldrack, R. A. Recovering meaning: left prefrontal cortex guides controlled semantic retrieval. *Neuron* **31,** 329–338 (2001).
25. Fu, S., Chen, Y., Smith, S., Iversen, S. & Matthews, P. M. Effects of word form on brain processing of written Chinese. *Neuroimage* **17,** 1538–1548 (2002).
26. Fiez, J. A. Sound and meaning: how native language affects reading strategies. *Nature Neurosci.* **3,** 3–5 (2000).
27. Kochunov, P. *et al.* Localized morphological brain differences between English speaking Caucasian and Chinese speaking Asian populations: New evidence of anatomical plasticity. *Neuroreport* **14,** 961–964 (2003).
28. Siok, W. T. & Fletcher, P. The role of phonological awareness and visual-orthographic skills in Chinese reading acquisition. *Dev. Psychol.* **36,** 887–899 (2001).
29. Snyder, P. J. & Harris, L. J. Handedness, sex, and familial sinistrality effects on spatial tasks. *Cortex* **29,** 115–134 (1993).
30. Talairach, J. & Tournoux, P. *Co-planar Stereotaxic Atlas of the Human Brain* (Thieme Medical Publishers, New York, 1988).
31. Fox, P. T. *et al.* A PET study of the neural system of stuttering. *Nature* **382,** 158–161 (1996).

Acknowledgements This work was supported by a Hong Kong Government RGC Central Allocation grant, and by the Intramural Research Program of NIMH. We thank J. Gabrieli, R. Desimone, C. K. Leong, K. K. Luke, S. Matthews and J. Spinks for support and comments.

Competing interests statement The authors declare that they have no competing financial interests.

Correspondence and requests for materials should be addressed to L.H.T. (lihaitan@intra.nimh.nih.gov).

Reading the Hedgehog morphogen gradient by measuring the ratio of bound to unbound Patched protein

Andreu Casali & Gary Struhl

Howard Hughes Medical Institute, Department of Genetics and Development, Columbia University, New York, New York 10032, USA

Morphogens are 'form-generating' substances that spread from localized sites of production and specify distinct cellular outcomes at different concentrations. A cell's perception of morphogen concentration is thought to be determined by the number of active receptors, with inactive receptors making little if any contribution[1]. Patched (Ptc)[2–5], the receptor for the morphogen Hedgehog (Hh)[6–12], is active in the absence of ligand and blocks the expression of target genes by inhibiting Smoothened (Smo), an essential transducer of the Hh signal[3,13–16]. Hh binding to Ptc abrogates the ability of Ptc to inhibit Smo, thereby unleashing Smo activity and inducing target gene expression[2,3,12–16]. Here, we show that a cell's measure of ambient Hh concentration is not determined solely by the number of active (unliganded) Ptc molecules. Instead, we find that Hh-bound Ptc can titrate the inhibitory action of unbound Ptc. Furthermore, we demonstrate that this effect is sufficient to allow normal reading of the Hh gradient in the presence of a form of Ptc that cannot bind the ligand[12] but retains its ability to inhibit Smo. These results support a model in which the ratio of bound to unbound Ptc molecules determines the cellular response to Hh.

Hh signal transduction is unusual in that the unbound receptor (Ptc) is the active form (that is, it keeps the pathway switched 'off' by inhibiting the transducer (Smo)). Binding by the ligand (Hh) inactivates the receptor, releasing Smo from inhibition and turning the pathway on[2,3,12–16]. The cell's perception of the amount of ambient Hh has been proposed to be determined solely by the number of unliganded (active) Ptc molecules[17]. Thus, as Hh rises from nil to peak concentrations, Smo activity would increase merely as a consequence of the progressive depletion of the pool of active Ptc protein. According to this depletion model, liganded Ptc would be functionally equivalent to the absence of Ptc. Alternatively, liganded Ptc might titrate the inhibitory activity of unliganded Ptc so that a cell's perception of Hh concentration would depend on the ratio of the two forms[12].

To distinguish these possibilities, we have expressed different levels of constitutively active $Ptc^{\Delta loop2}$ protein, a deleted form of Ptc (Fig. 1a) that cannot bind Hh but can still repress Smo[12], and asked whether the minimum amount of $Ptc^{\Delta loop2}$ necessary to shut down the pathway depends on the presence of liganded Ptc. In the simple depletion model, in which Hh binding merely inactivates Ptc, $Ptc^{\Delta loop2}$ should be impervious to liganded Ptc, and the minimum amount of $Ptc^{\Delta loop2}$ required to turn off the pathway should not change. In the titration model, the presence of liganded Ptc should counteract the inhibitory activity of $Ptc^{\Delta loop2}$, requiring higher levels of $Ptc^{\Delta loop2}$ to keep the pathway off.

Three Flp-out transgenes[6] called $L > P^{\Delta 2}$, $M > P^{\Delta 2}$ and $H > P^{\Delta 2}$ (Fig. 1b; see Methods) were used to express low, medium or high levels of $Ptc^{\Delta loop2}$ protein in clones of imaginal wing disc cells (Fig. 1b; see Methods). Wing discs are subdivided into anterior and posterior compartments, with cells in the posterior compartment programmed to express and those in the anterior compartment to respond to Hh[6–9,18]. Ptc is normally expressed in anterior compartment cells only at low levels, except in those anterior cells that are located close to the anteroposterior compartment boundary

where Ptc expression is markedly upregulated by Hh[2,7,8,16,19,20] (Fig. 1c). To quantify Ptc$^{\Delta loop2}$ expression generated by each transgene, we measured the amount of Ptc staining in posterior compartment clones in the wing imaginal disc relative to the basal level of endogenous Ptc expressed in anterior cells away from the compartment boundary (defined as 100%; see Methods). $L > P^{\Delta 2}$, $M > P^{\Delta 2}$ and $H > P^{\Delta 2}$ clones in the posterior compartment expressed levels of Ptc$^{\Delta loop2}$ that were approximately 80%, 140% and 320%, respectively, of the basal level (Fig. 1c), well within the physiological range of Ptc expression, which normally peaks at around 700% in anterior cells that abut the boundary.

To examine the consequences of expressing each transgene on Hh transduction, we assayed two target genes, *decapentaplegic* (*dpp*) and *collier* (*col*; also known as *knot*), which are induced by low and high thresholds of Hh signalling, respectively. *dpp*, monitored using a *dpp–lacZ* gene, is normally expressed in a broad stripe of approximately 15–20 cell diameters that has a sharp peak at the compartment boundary and declines anteriorly as a function of distance from the posterior compartment[6–8,12]. In contrast, *col*, monitored by the presence of Col protein, is expressed in a narrower band of around 5–10 cells[21]. $L > P^{\Delta 2}$ clones had no effect on Hh transduction (Fig. 2a), except at the extreme, anterior limit of the *dpp–lacZ* domain where *dpp–lacZ* expression was blocked in cells that would otherwise express barely detectable levels (data not shown). $M > P^{\Delta 2}$ clones showed a more readily detectable effect, generally reducing the level of *dpp–lacZ* and Col expression (Fig. 2b). By contrast, $H > P^{\Delta 2}$ clones were completely refractory to Hh: they failed to express either *dpp–lacZ* or Col even when located next to the compartment boundary (Fig. 2c).

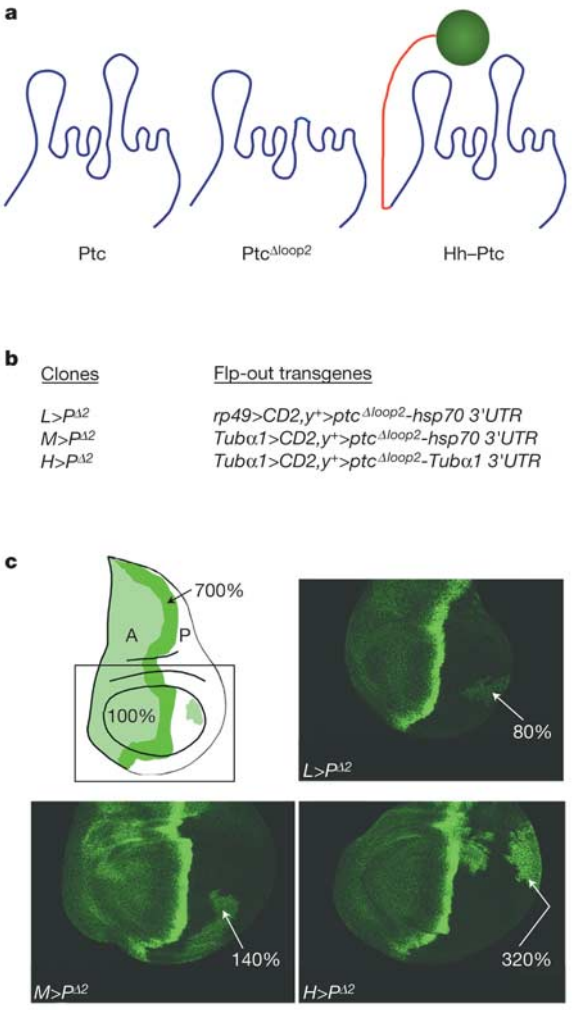

Figure 1 Generation of clones expressing low ($L > P^{\Delta 2}$), medium ($M > P^{\Delta 2}$) and high ($H > P^{\Delta 2}$) levels of Ptc$^{\Delta loop2}$. **a**, Ptc[16,19,20] protein and the two modified versions, Ptc$^{\Delta loop2}$ (ref. 12) and Hh–Ptc (see Methods), used in this study. **b**, Flp-out transgenes used to generate clones of $L > P^{\Delta 2}$, $M > P^{\Delta 2}$ and $H > P^{\Delta 2}$ cells by Flp-mediated recombination of the $> CD2,y^+ >$ cassette (Methods). **c**, Wing imaginal discs bearing posterior compartment Flp-out clones of $L > P^{\Delta 2}$, $M > P^{\Delta 2}$ and $H > P^{\Delta 2}$ cells stained for Ptc protein. The average level of expression of $L > P^{\Delta 2}$, $M > P^{\Delta 2}$ and $H > P^{\Delta 2}$ was approximately 80% ($n = 6$; s.d. = 19%), 140% ($n = 9$; s.d. = 22%) and 320% ($n = 12$; s.d. = 41%), respectively, relative to the basal level of endogenous Ptc staining in anterior compartment cells away from the anteroposterior compartment boundary (see Methods). The peak level of endogenous Ptc staining in anterior cells abutting the compartment boundary was ~700% ($n = 12$; s.d. = 165%).

To determine whether the same, high level of Ptc$^{\Delta loop2}$ expression is necessary to block Hh pathway activity in the absence of endogenous Ptc, we generated clones of $L > P^{\Delta 2}$, $M > P^{\Delta 2}$ and $H > P^{\Delta 2}$ cells that were also *ptc*$^-$ (see Methods). *dpp–lacZ* and Col are constitutively expressed in *ptc*$^-$ cells; however, both responses were completely blocked when these cells expressed any one of the three transgenes (Fig. 2d and data not shown). This effect is particularly notable in the case of the $L > P^{\Delta 2}$ transgene because its expression has virtually no effect on Hh transduction in otherwise wild-type cells. Indeed, entirely $L > P^{\Delta 2}$ animals survive as phenotypically normal adults (Fig. 2e); however, $L > P^{\Delta 2}$ animals differ from wild-type animals in that Hh transduction is blocked, rather than constitutively activated, in clones of *ptc*$^-$ cells (Fig. 2e–g). This result confirms that Hh transduction in $L > P^{\Delta 2}$ cells depends on the presence of both Hh and endogenous Ptc: in the absence of either (for example, in anterior cells located away from the compartment boundary, or in *ptc*$^-$ cells located anywhere within the anterior compartment) the Hh transduction pathway is off. We therefore infer that in $L > P^{\Delta 2}$ cells liganded Ptc is not equivalent to the absence of Ptc; instead, it is responsible in this context for normal activation of the Hh pathway. This result indicates that liganded Ptc titrates the inhibitory activity of unliganded Ptc$^{\Delta loop2}$, and hence that it is the ratio of liganded to unliganded Ptc molecules rather than the absolute number of unliganded Ptc molecules that determines the Hh response.

As a further test of these conclusions, we examined $M > P^{\Delta 2}$ clones in the posterior compartment, where cells normally make and are exposed to uniformly high levels of Hh, and where Smo is constitutively active owing to the absence of endogenous Ptc[22–24]. To assay Ptc activity in this context, we expressed a green fluorescent protein (GFP)-tagged, functionally inactive form of the transcription factor Cubitus interruptus (CiΔZnGFP; Fig. 3a). Ci is normally stabilized and activated in response to Hh[25–27]. When CiΔZnGFP is expressed throughout the presumptive wing blade it is stabilized in all posterior compartment cells in response to the unfettered activity of Smo (Fig. 3a). Posterior compartment clones of $M > P^{\Delta 2}$ cells destabilize CiΔZnGFP (Fig. 3b), as expected because Ptc$^{\Delta loop2}$ cannot bind Hh and constitutively inhibits Smo. However, when these clones carried a second transgene, $M > P^{+}$, that expresses Ptc$^+$ in the posterior compartment[3], the CiΔZnGFP protein is once again stabilized (Fig. 3c). Because Hh is normally expressed at peak levels in cells of the posterior compartment, we infer that some if not most of the ectopic Ptc$^+$ protein expressed in the posterior compartment is bound by Hh. Hence, as in the anterior compartment, it seems that liganded Ptc can drive Hh transduction in the presence of constitutively active Ptc$^{\Delta loop2}$ that would otherwise shut down the pathway.

To estimate the range of ratios between unliganded and liganded Ptc that may normally distinguish between off and on states of the Hh pathway, we performed a titration experiment in which we generated clones of *ptc*$^-$ cells expressing different ratios of constitutively unliganded Ptc (Ptc$^{\Delta loop2}$) and Hh–Ptc, a chimaeric protein that seems to behave like a constitutively liganded form of Ptc (Fig. 1a; see Methods).

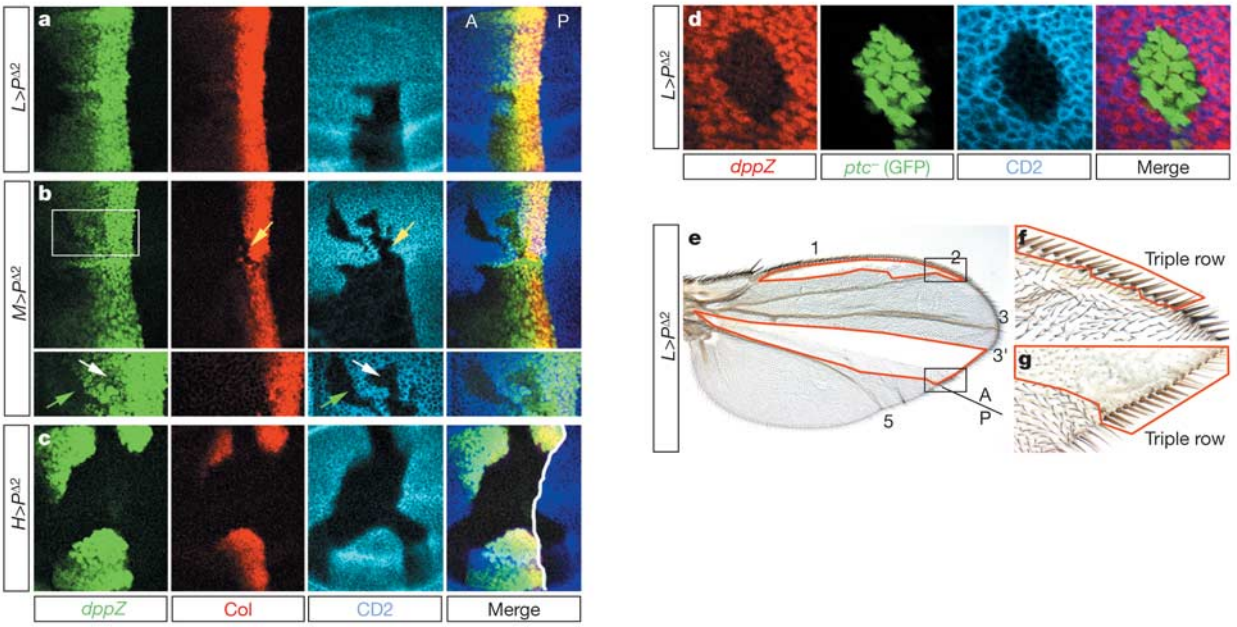

Figure 2 Different amounts of Ptc$^{\Delta loop2}$ are required to inhibit the Hh pathway depending on the presence or absence of endogenous Ptc. **a**–**c**, Wing discs bearing Flp-out clones of $L > P^{\Delta 2}$ (**a**), $M > P^{\Delta 2}$ (**b**) and $H > P^{\Delta 2}$ (**c**) cells in the anterior compartment, marked black by the absence of CD2 staining (blue). The anteroposterior (A–P) compartment boundary is marked by the sharp border of *dpp–lacZ* (*dppZ*; green) and Collier (Col; red) expression in **a** and **b**, and by a white line in **c** (anterior to the left). Expression of *dpp–lacZ* and Col appear normal in $L > P^{\Delta 2}$ clones, but are reduced or abolished in $M > P^{\Delta 2}$ and $H > P^{\Delta 2}$ clones. In the boxed region of **b** (magnified in the bottom panels), white and green arrows mark, respectively, reduced or abolished expression of *dpp–lacZ*; the yellow arrow in the main panel marks the absence of Col expression. **d**, Low level Ptc$^{\Delta loop2}$ expression ($L > P^{\Delta 2}$) in an anterior compartment clone of *ptc* $^-$ cells close to the compartment boundary (*ptc* $^-$ genotype marked by the presence of GFP (green)). The $L > P^{\Delta 2}$ genotype is marked black by the absence of CD2 (blue); *dpp–lacZ* expression is repressed. **e**, Two anterior compartment clones of *ptc* $^-$ cells (outlined in red) in a wing in which all cells carry the flipped-out $L > P^{\Delta 2}$ transgene (veins 1, 2, 3 and 5, as well as the anteroposterior compartment boundary are indicated where they abut the wing margin); both clones behave as if mutant for *smo*. The anteriorly situated clone (top) is phenotypically wild type, indicating that the Hh transduction pathway is off. The clone along the anteroposterior compartment boundary (bottom) forms a mirror symmetric duplication of a more anterior pattern, including an ectopic vein 3 (3′) and triple row bristles (**g**), at the expense of posterior compartment pattern (vein 4 is absent). As in the case of *smo* $^-$ clones, this distinctive phenotype reflects the failure of the mutant cells to transduce and sequester Hh, displacing the source of Dpp signalling to the middle of the anterior compartment (see refs 3, 12). **f**, **g**, Details of the boxed portions in **e**, showing, respectively, normal and ectopic 'triple row' bristles formed by *ptc* $^-$ cells, confirming that the Hh transduction pathway is off (clones are marked by *yellow*, which lightens bristle colour (**f**, **g**), and *shavenoid*, which removes hairs (**g**); the red outlines in **e** show the contribution of the clones to the dorsal surface; only those portions of the wing in which both the dorsal and ventral surfaces are mutant appear hairless in this image).

We generated two transgenes, $L >$ *hh–ptc* and $H >$ *hh–ptc*, and quantified their expression level as 50% and 220% relative to endogenous Ptc in anterior cells not exposed to Hh (Fig. 4 legend). By activating different combinations of $L > P^{\Delta 2}$, $M > P^{\Delta 2}$, $L >$ *hh–ptc* and $H >$ *hh–ptc* transgenes in anterior compartment clones of *ptc* $^-$ cells, we generated cells in which the only Ptc proteins present are Hh–Ptc and Ptc$^{\Delta loop2}$, at ratios of 220%:80% ($H >$ *hh–ptc*:$L > P^{\Delta 2}$), 220%:140% ($H >$ *hh–ptc*:$M > P^{\Delta 2}$) or 50%:80% ($L >$ *hh–ptc*:$L > P^{\Delta 2}$). Both *dpp–lacZ* and Col expression were fully activated at the highest ratio of Hh–Ptc:Ptc$^{\Delta loop2}$ (220%:80%; Fig. 4a, b); however, neither was expressed in cells in which the ratio was reduced, either by an approximately twofold increase in the level of Ptc$^{\Delta loop2}$ (220%:140%; Fig. 4c and data not shown), or by an approximately fourfold decrease in the level of Hh–Ptc (50%:80%; Fig. 4d and data not shown). Thus, as little as an approximately twofold change in the ratio of Hh–Ptc:Ptc$^{\Delta loop2}$ seems to be sufficient to distinguish between on and off states of the pathway. We note that the total amount of Ptc protein in these clones falls within a range of ~130–360% relative to the basal level of endogenous Ptc, well below the level of peak Ptc expression induced by Hh in anterior cells abutting the posterior compartment (~700%). The range in the amount of Ptc corresponds to the moderately elevated levels of endogenous Ptc that are present normally in cells responding to intermediate levels of Hh signal. Hence, relatively small (on the scale of a few fold) differences in the ratio of liganded:unliganded Ptc may be sufficient to control the full range of responses to the Hh gradient under physiologically relevant conditions.

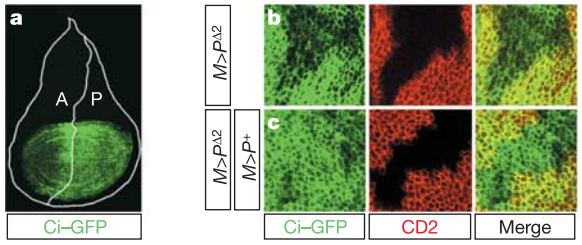

Figure 3 Inhibition of Hh transduction by Ptc$^{\Delta loop2}$ is blocked by co-expression of Ptc$^+$ and Hh. **a**, CiΔZnGFP (Ci–GFP, green) expressed throughout the wing pouch under the control of *nubbin–Gal4* is destabilized in anterior compartment cells away from the compartment boundary. **b**, $M > P^{\Delta 2}$ clone (marked black by the absence of CD2 (red)) in the posterior compartment where endogenous Ptc is not expressed: Ci–GFP is destabilized. **c**, $M > P^{\Delta 2}$ clone, similarly marked, in the posterior compartment of a wing disc expressing Ptc$^+$ from a $M > P^+$ transgene[3]: Ci–GFP is not destabilized.

We note that our results differ from those of Taipale *et al*[17], who found that overexpressing mPtc$^+$ and mPtc$^{\Delta loop2}$ in a 3:1 ratio in mammalian tissue culture cells exposed to a soluble amino-terminal form of Sonic Hh (Shh-N) failed to activate target gene expression. However, the actual ratio of liganded to unliganded forms of mPtc

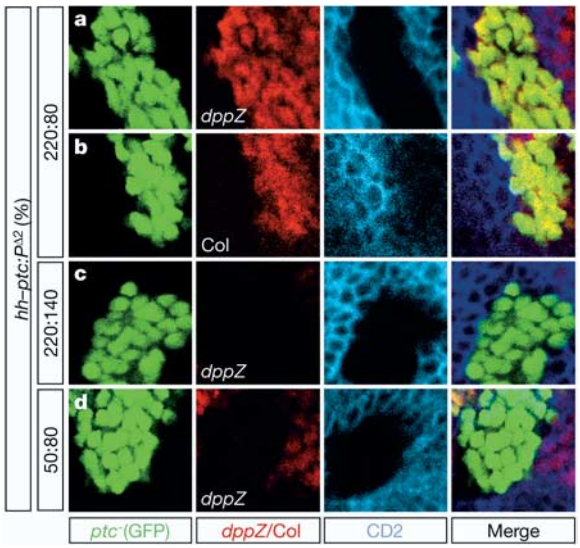

Figure 4 Estimating the change in the ratio of liganded to unliganded Ptc necessary to distinguish on and off states of the Hh transduction pathway. **a**–**d**, Anterior compartment clones of *ptc*$^-$ cells (marked by the presence of GFP (green)) expressing given combinations of $L > P^{\Delta 2}$ or $M > P^{\Delta 2}$ and $L >$ *hh–ptc* or $H >$ *hh–ptc* (marked black by the absence of CD2 staining (blue)) were monitored for the expression of *dpp–lacZ* (**a**, **c**, **d**; red) or Col (**b**; red). **a**, **b**, *dpp–lacZ* (**a**) and Col (**b**) are both strongly expressed in *ptc*$^-$ cells co-expressing high levels of Hh–Ptc ($H >$ *hh–ptc*, ~220%; $n = 7$; s.d. = 44%) and low levels of Ptc$^{\Delta loop2}$ ($L > P^{\Delta 2}$, ~80%). **c**, Increasing the level of Ptc$^{\Delta loop2}$ from low (~80%) to medium ($M > P^{\Delta 2}$, ~140%) while holding the high level of Hh–Ptc (~220%) constant was sufficient to inhibit the pathway in *ptc*$^-$ cells, as shown by the absence of *dpp–lacZ* expression. **d**, Decreasing the level of Hh–Ptc from high (~220%) to low ($L >$ *hh–ptc*, ~50%; $n = 8$; s.d. = 11%) while holding the low level (~80%) of Ptc$^{\Delta loop2}$ expression constant also resulted in inhibition of the pathway in *ptc*$^-$ cells (*dpp–lacZ* expression is no longer detected).

obtained in this experiment was not determined; if as little as one-fifth of the available mPtc$^+$ remained unliganded, the ratio of liganded to unliganded forms of mPtc protein would be 3:2, which our present results (Fig. 4c) suggest may be inadequate to activate Hh target genes under normal conditions. It is also unclear whether the ratio of liganded to unliganded Ptc necessary to activate the pathway will be the same in all biological contexts, or when the total amount of Ptc protein is well above peak physiological levels, as is likely in the tissue culture experiments.

How might the ratio of liganded to unliganded Ptc determine the level of Smo activity? Unliganded Ptc might function catalytically to inhibit Smo[16,17,22–24], and the presence of liganded Ptc would titrate or counterbalance the catalytic activity of unliganded Ptc. For example, unliganded Ptc might function as a transporter to drive the cytosolic accumulation of a Smo antagonist[17], and liganded Ptc might allow some antagonist to translocate in the opposite direction. Alternatively, liganded and unliganded Ptc might function stoichiometrically by competing for access to Smo (or a Smo effector) and exerting opposing effects on its activity[12,16]. Another possibility is that Ptc exists as a higher-order multimer (for example, as a trimer), as proposed for the structurally related AcrB transporter[28]. In this model, binding of Hh to one monomer in any given multimer might block the ability of that multimer to function catalytically to inhibit Smo, or interfere with the activity of the remaining monomers, for example, by targeting the multimer for degradation.

A conserved feature of Hh signalling is that, during normal development, high levels of Hh signalling upregulate *ptc* transcription[16]. This generates a sharp peak of Ptc accumulation[2,7,8,19,20] (Fig. 1c) that has an essential role in sequestering Hh and limiting its spread into responsive tissue[3,12]. A ratiometric mechanism that involves titration of the inhibitory action of unliganded Ptc by liganded Ptc might allow cells close to the source of Hh to upregulate sufficiently high levels of Ptc in order to impede effectively the movement of Hh without suppressing the response of these same cells to Hh by the inhibitory action of any residual unbound Ptc. Our present results suggest that as the gradient of Hh declines from peak levels to nil, the level of Smo activity, and hence the cell's perception of ambient Hh, will depend on the ratio of liganded to unliganded Ptc, which in turn will depend on the absolute amount of Ptc. In regions away from the Hh source, where Ptc is upregulated weakly or not at all, titration of unbound Ptc by Hh-bound Ptc might also be necessary for cells to detect and respond appropriately to low levels of ambient Hh. □

Methods

Immunostaining

Immunostaining was performed using standard techniques with antibodies against Ptc (I. Guerrero[8]), CD2 (Serotec), βgal (Cappel) and Col (A. Vincent[21]).

Mutations and transgenes used

Unless otherwise stated, all mutations and transgenes have been described previously, or were derived by combining well-defined components of previously described transgenes (see refs 3, 6, 12, 29). The $H > P^{\Delta 2}$ transgene was generated *in vivo* by Flp-mediated recombination of a *Tubα1* $>$ *CD2,y*$^+$ $>$ *ptc*$^{\Delta loop2}$ transgene containing the ubiquitously expressed *Tubulinα1* (*Tubα1*) promoter: recombination excises the $>$ *CD2,y*$^+$ $>$ Flp-out cassette to create clones of *Tubα1* $>$ *ptc*$^{\Delta loop2}$ ($H > P^{\Delta 2}$) cells, which express Ptc$^{\Delta loop2}$ instead of the reporter protein CD2. The $M > P^{\Delta 2}$ and $L > P^{\Delta 2}$ transgenes were generated similarly. The $M > P^{\Delta 2}$ transgene differs from $H > P^{\Delta 2}$ in using the *hsp70* 3′ untranslated region (UTR), which is ~two–threefold less stable than the *Tubα1* 3′UTR used in $H > P^{\Delta 2}$ (ref. 29); the $L > P^{\Delta 2}$ transgene differs from $M > P^{\Delta 2}$ in using the *ribosomal protein 49* (*rp49*) promoter (which is ~twofold weaker than the *Tubα1* promoter)[29] (Fig. 1b). Flp-out and mitotic recombination clones were generated using standard techniques (for example, as in refs 3, 6, 30); multiple heat shocks were given during the first instar to generate clones within clones (as in Figs 2d and 4).

The *ciΔZnGFP* sequence encodes an inactive form of Ci, lacking the third and fourth zinc fingers (deleted between Pro 498 and Ser 594), fused to GFP at the carboxy terminus, and is expressed under Gal4/UAS control.

The Hh–Ptc protein is composed of the N-terminal signalling portion of Hh (amino acids 1–256) joined via three haemagglutinin (HA) tags to the juxtamembrane and transmembrane domains of the receptor Sevenless (Sev), joined to the N terminus of full-length Ptc (Fig. 1a; HA–Sev and Sev–Ptc joins are, respectively, ISSHVH–LST and LVRK–rrsgsls–RDSLP; with linker peptide in lower case). Hh–Ptc behaves as a constitutively liganded form of Ptc by the following criteria (data not shown). First, overexpression of Hh–Ptc does not rescue the absence of endogenous Ptc (expected, as Hh–Ptc should be self-inactivated; genotype: *y w hsp70–flp UAS–GFPnls; FRT42D ptc*^{IIW}*/ dpp–lacZ*^{10628} *FRT42D Tubα1–Gal80; UAS–hh–ptc/Tubα1–Gal4*). Second, overexpression of Hh–Ptc ectopically activates the Hh transduction pathway in otherwise wild-type cells in the wing primordium (expected if Hh–Ptc titrates the inhibitory action of endogenous, unliganded Ptc; genotype: *y w hsp70–flp UAS–GFPnls; dpp–lacZ*^{10628}*/+; UAS–hh–ptc/ Tuba1* $>$ *CD2,y*$^+$ $>$ *Gal4*). In contrast, clones similarly overexpressing a deleted form of Hh–Ptc lacking the Hh signalling domain do not activate the Hh transduction pathway (expected if the Hh signalling domain is responsible for inactivating Ptc within the Hh–Ptc chimaera). Third, clones overexpressing Hh–Ptc constitutively activate the Hh pathway in a strictly cell autonomous fashion (expected if the Hh domain is sequestered by the Ptc protein to which it is fused and not available to bind Ptc on neighbouring cells; genotype as in the second criterion). In contrast, clones similarly overexpressing a deleted form of Hh–Ptc that lacks the second extracellular loop (Hh–Ptc$^{\Delta loop2}$) activate the Hh pathway in neighbouring cells (expected, as the attached Hh signalling domain should be available to signal to neighbouring cells because it cannot be bound by Ptc$^{\Delta loop2}$ in the Hh–Ptc$^{\Delta loop2}$ chimaera).

Expression level quantification

For each posterior compartment clone of $L > P^{\Delta 2}$, $M > P^{\Delta 2}$ and $H > P^{\Delta 2}$ cells, the level of Ptc$^{\Delta loop2}$ expression relative to the basal level of endogenous Ptc expression in the anterior compartment was determined by averaging the intensity of five samples of 35 pixels each within (1) the clone; (2) the anterior compartment far from the compartment boundary; and (3) portions of the posterior compartment not containing the clone. The resulting levels of staining in the clone (1) and in the anterior compartment (2) were normalized by subtracting the background level of staining (3); the level of staining in the clone is expressed as the per cent of the level of basal staining in the anterior compartment. All measurements were made within the wing primordium and staining intensity was quantified using ImageJ 1.25 (Rasband, W. S., http://rsb.info.nih.gov/ij/). To validate the method, we quantified the levels of Ptc staining in 2 × *ptc*$^+$ clones relative to surrounding 1 × *ptc*$^+$ (*FRT42 ptc*^{IIW}*/FRT42 arm–lacZ*) tissue (normalizing the level of staining by subtracting the level of staining detected in the 0 × *ptc*$^+$ 'twin-spot' clones): the level of Ptc expression in 1 × *ptc*$^+$ cells was 51% ($n = 5$; s.d. = 15%) that of neighbouring 2 × *ptc*$^+$ cells. We also quantified Ptc staining in anterior compartment clones of $M > P^{\Delta 2}$ cells. The measurement obtained, 210% ($n = 4$; s.d. = 22%), corresponds approximately to the

sum of Ptc staining in $M > P^{42}$ posterior compartment clones and the basal level of Ptc staining in anterior compartment cells (Fig. 1 legend), validating our use of posterior compartment clones to quantify $Ptc^{\Delta loop2}$ expression in sibling clones in the anterior compartment.

Genotypes

We used the following *Drosophila* genotypes. Figures 1 and 2a–c: *y w hsp70–flp; +* (or *dpp–lacZ*^{10628}*)/+; Tubα1* (or *rp49*) *> CD2,y*$^{+}$ *> ptc*$^{\Delta loop2}$*–Tubα1 3′UTR* (or *hsp70 3′UTR*)*/+*. Figure 2d: *y w hsp70–flp UAS–GFPnls; FRT42D ptc*^{IIW}*/dpp–lacZ*^{10628} *FRT42D Tubα1–Gal80; rp49 > CD2,y*$^{+}$ *> ptc*$^{\Delta loop2}$*–hsp70 3′UTR/Tubα1–Gal4*. Figure 2e–g: *y w hsp70–flp; FRT42D ptc*^{IIW} *sha/FRT42 P(w*$^{+}$ *ptc*$^{+}$*) P(hsp70–CD2,y*$^{+}$*); rp49 > ptc*$^{\Delta loop2}$*–hsp70 3′UTR/+*. *P(w*$^{+}$ *ptc*$^{+}$*)*, a gift from J. Hooper, contains a ~20-kilobase genomic fragment from the *ptc* locus that confers partial rescuing activity. Figure 3: *y w hsp70–flp; nub–Gal4 UAS–ciΔZnGFP/+; Tubα1 > CD2,y*$^{+}$ *> ptc*$^{\Delta loop2}$*–hsp70 3′UTR/+* (or *Tubα1 > ptc*$^{+}$*–hsp70 3′UTR*). Figure 4: *y w hsp70–flp UAS–GFPnls; rp49* (or *Tubα1) > CD2,y*$^{+}$ *> ptc*$^{\Delta loop2}$*–hsp70 3′UTR FRT42D ptc*^{IIW}*/dpp–lacZ*^{10628} *FRT42D Tubα1–Gal80; Tubα1 > CD2,y*$^{+}$ *> hh–ptc–Tubα1 3′UTR* (or *rp49 > CD2,y*$^{+}$ *> hh–ptc–hsp70 3′UTR)/Tubα1–Gal4*.

Received 12 February; accepted 9 July 2004; doi:10.1038/nature02835.
Published online 8 August 2004.

1. Gurdon, J. B. & Bourillot, P. Y. Morphogen gradient interpretation. *Nature* **413,** 797–803 (2001).
2. Ingham, P. W., Taylor, A. M. & Nakano, Y. Role of the *Drosophila* patched gene in positional signalling. *Nature* **353,** 184–187 (1991).
3. Chen, Y. & Struhl, G. Dual roles for patched in sequestering and transducing Hedgehog. *Cell* **87,** 553–563 (1996).
4. Stone, D. M. *et al.* The tumour-suppressor gene patched encodes a candidate receptor for Sonic hedgehog. *Nature* **384,** 129–134 (1996).
5. Marigo, V., Davey, R. A., Zuo, Y., Cunningham, J. M. & Tabin, C. J. Biochemical evidence that patched is the Hedgehog receptor. *Nature* **384,** 176–179 (1996).
6. Basler, K. & Struhl, G. Compartment boundaries and the control of *Drosophila* limb pattern by hedgehog protein. *Nature* **368,** 208–214 (1994).
7. Tabata, T. & Kornberg, T. B. Hedgehog is a signaling protein with a key role in patterning *Drosophila* imaginal discs. *Cell* **76,** 89–102 (1994).
8. Capdevila, J., Estrada, M. P., Sanchez-Herrero, E. & Guerrero, I. The *Drosophila* segment polarity gene patched interacts with decapentaplegic in wing development. *EMBO J.* **13,** 71–82 (1994).
9. Struhl, G., Barbash, D. A. & Lawrence, P. A. Hedgehog organises the pattern and polarity of epidermal cells in the *Drosophila* abdomen. *Development* **124,** 2143–2154 (1997).
10. Mullor, J. L., Calleja, M., Capdevila, J. & Guerrero, I. Hedgehog activity, independent of decapentaplegic, participates in wing disc patterning. *Development* **124,** 1227–1237 (1997).
11. Strigini, M. & Cohen, S. M. A Hedgehog activity gradient contributes to AP axial patterning of the *Drosophila* wing. *Development* **124,** 4697–4705 (1997).
12. Briscoe, J., Chen, Y., Jessell, T. M. & Struhl, G. A hedgehog-insensitive form of patched provides evidence for direct long-range morphogen activity of sonic hedgehog in the neural tube. *Mol. Cell* **7,** 1279–1291 (2001).
13. Hooper, J. E. Distinct pathways for autocrine and paracrine Wingless signalling in *Drosophila* embryos. *Nature* **372,** 461–464 (1994).
14. van den Heuvel, M. & Ingham, P. W. smoothened encodes a receptor-like serpentine protein required for hedgehog signalling. *Nature* **382,** 547–551 (1996).
15. Alcedo, J., Ayzenzon, M., Von Ohlen, T., Noll, M. & Hooper, J. E. The *Drosophila* smoothened gene encodes a seven-pass membrane protein, a putative receptor for the hedgehog signal. *Cell* **86,** 221–232 (1996).
16. Ingham, P. W. & McMahon, A. P. Hedgehog signaling in animal development: paradigms and principles. *Genes Dev.* **15,** 3059–3087 (2001).
17. Taipale, J., Cooper, M. K., Maiti, T. & Beachy, P. A. Patched acts catalytically to suppress the activity of Smoothened. *Nature* **418,** 892–897 (2002).
18. Lawrence, P. A. & Struhl, G. Morphogens, compartments, and pattern: lessons from *Drosophila? Cell* **85,** 951–961 (1996).
19. Nakano, Y. *et al.* A protein with several possible membrane-spanning domains encoded by the *Drosophila* segment polarity gene patched. *Nature* **341,** 508–513 (1989).
20. Hooper, J. E. & Scott, M. P. The *Drosophila* patched gene encodes a putative membrane protein required for segmental patterning. *Cell* **59,** 751–765 (1989).
21. Vervoort, M., Crozatier, M., Valle, D. & Vincent, A. The COE transcription factor Collier is a mediator of short-range Hedgehog-induced patterning of the *Drosophila* wing. *Curr. Biol.* **9,** 632–639 (1999).
22. Alcedo, J., Zou, Y. & Noll, M. Posttranscriptional regulation of smoothened is part of a self-correcting mechanism in the Hedgehog signaling system. *Mol. Cell* **6,** 457–465 (2000).
23. Denef, N., Neubuser, D., Perez, L. & Cohen, S. M. Hedgehog induces opposite changes in turnover and subcellular localization of patched and smoothened. *Cell* **102,** 521–531 (2000).
24. Ingham, P. W. *et al.* Patched represses the Hedgehog signalling pathway by promoting modification of the Smoothened protein. *Curr. Biol.* **10,** 1315–1318 (2000).
25. Hepker, J., Wang, Q. T., Motzny, C. K., Holmgren, R. & Orenic, T. V. *Drosophila* cubitus interruptus forms a negative feedback loop with patched and regulates expression of Hedgehog target genes. *Development* **124,** 549–558 (1997).
26. Aza-Blanc, P. & Kornberg, T. B. Ci: a complex transducer of the hedgehog signal. *Trends Genet.* **15,** 458–462 (1999).
27. Methot, N. & Basler, K. Hedgehog controls limb development by regulating the activities of distinct transcriptional activator and repressor forms of Cubitus interruptus. *Cell* **96,** 819–831 (1999).
28. Murakami, S., Nakashima, R., Yamashita, E. & Yamaguchi, A. Crystal structure of bacterial multidrug efflux transporter AcrB. *Nature* **419,** 587–593 (2002).
29. Greenwood, S. & Struhl, G. Different levels of Ras activity can specify distinct transcriptional and morphological consequences in early *Drosophila* embryos. *Development* **124,** 4879–4886 (1997).
30. Lee, T. & Luo, L. Mosaic analysis with a repressible cell marker for studies of gene function in neuronal morphogenesis. *Neuron* **22,** 451–461 (1999).

Acknowledgements We thank A. Adachi for generating transgenic flies; X.-J. Qiu for technical assistance; and R. Axel, E. Gouaux, I. Greenwald, T. Jessell, L. Johnston, R. Mann and A. Tomlinson for discussion and advice on the manuscript. A.C. is a Postdoctoral Associate and G.S. is an Investigator of the Howard Hughes Medical Institute.

Competing interests statement The authors declare that they have no competing financial interests.

Correspondence and requests for materials should be addressed to G.S. (gs20@columbia.edu).

Netrin-1 controls colorectal tumorigenesis by regulating apoptosis

Laetitia Mazelin[1], Agnès Bernet[1]*, Christelle Bonod-Bidaud[1]*, Laurent Pays[1], Ségolène Arnaud[1], Christian Gespach[2], Dale E Bredesen[3], Jean-Yves Scoazec[4] & Patrick Mehlen[1,5]

[1]*Apoptosis/Differentiation Laboratory—Equipe labellisée 'La Ligue'—Molecular and Cellular Genetic Center, CNRS UMR 5534, University of Lyon, 69622 Villeurbanne, France*
[2]*INSERM U482, Signal Transduction and Cellular Functions in Diabetes and Digestive Cancers, Hospital Saint-Antoine, 75571 Paris, France*
[3]*The Buck Institute for Age Research, Novato, California 94945, USA*
[4]*INSERM U45 and ANIPATH, IFR62, Faculté Laennec, 69437 Lyon, France*
[5]*Centre Leon Bérard, 69373 Lyon, France*

* These authors contributed equally to this work.

The expression of the protein DCC (deleted in colorectal cancer) is lost or markedly reduced in numerous cancers and in the majority of colorectal cancers due to loss of heterozygosity in chromosome 18q, and has therefore been proposed to be a tumour suppressor[1]. However, the rarity of mutations found in DCC, the lack of cancer predisposition of DCC mutant mice, and the presence of other tumour suppressor genes in 18q have raised doubts about the function of DCC as a tumour suppressor[2]. Unlike classical tumour suppressors, DCC has been shown to induce apoptosis conditionally: by functioning as a dependence receptor, DCC induces apoptosis unless DCC is engaged by its ligand, netrin-1 (ref. 3). Here we show that inhibition of cell death by enforced expression of netrin-1 in mouse gastrointestinal tract leads to the spontaneous formation of hyperplastic and neoplastic lesions. Moreover, in the adenomatous polyposis coli mutant background associated with adenoma formation, enforced expression of netrin-1 engenders aggressive adenocarcinomatous malignancies. These data demonstrate that netrin-1 can promote intestinal tumour development, probably by regulating cell survival. Thus, a netrin-1 receptor or receptors function as conditional tumour suppressors.

Netrin-1, a diffusible laminin-related protein, is a bifunctional molecule. It has a major role during nervous system development in mediating chemo-attraction and chemo-repulsion of axons and neurons by interacting with its main receptor, DCC (refs 4, 5, 6). However, netrin-1 has also been described recently as a survival factor. Indeed, the netrin-1 receptors DCC and UNC5H (that is, UNC5H1, UNC5H2 and UNC5H3) belong to the so-called dependence receptor family[3,7]. Such receptors, which also include RET (rearranged during transfection)[8], β-integrins[9], Patched[10] and the p75 neurotrophin receptor (p75NTR)[11], share the functional property of inducing cell death when disengaged from their ligands but not when bound by their ligands. Such receptors thus create cellular states of dependence on their respective ligands[12,13].